Monitoring of tritium and impurities in the first wall of fusion devices using a LIBS based diagnostic

H. J. VAN DER MEIDEN
DIFFER, De Zaale 20, NL-5612 AJ Eindhoven, Netherlands
h.j.vandermeiden@differ.nl

S. ALMAVIVA, G. MADDALUNO
ENEA, Italian National Agency for New Technologies, Via Enrico Fermi, 45, 00040, Frascati, Italy

J. BUTIKOVA
Institute of Solid State Physics, University of Latvia, Ķengaraga iela 8, Rīga LV-1063, Latvia

V. DWIVEDI, A. MARÍN ROLDÁN, M. PISARČÍK, M. VEIS, P.VEIS
Dept. of Exp. Physics, FMPI, Comenius University, Mlynská dolina F2, 842 48 Bratislava, Slovakia

P. GASIOR, W. GROMELSKI, M. KUBKOWSKA
IPPLM Institute of Plasma Physics and Laser Microfusion, Hery Street 23, 01-497, Warsaw, Poland

A. HAKOLA
VTT, P.O.Box 1000, 02044 VTT, Finland

X. JIANG, G. SERGIENKO, S. BREZINSEK
Forschungszentrum Jülich, Institut für Energie- und Klimaforschung – Plasmaphysik Jülich, Germany

I. JÕGI, P. PARIS, K. PIIP, M. Laan
Institute of Physics, University of Tartu, W. Ostwaldi 1, 50411, Tartu, Estonia

J. KARHUNEN
Aalto University, Dept. of Applied Physics, P.O. Box 11100, 00076 Aalto, Finland

EUROfusion WP PFC Contributors* *www.euro-fusionscipub.org/PFC*
*See the author list of S. Brezinsek et al. 2017 Nucl. Fusion 57 116041.

 © xxxx IOP Publishing Ltd

Monitoring of tritium and impurities in the first wall of fusion devices using a LIBS based diagnostic

H.J. van der Meiden[1], S. Almaviva[2], J. Butikova[3], V. Dwivedi[4], P. Gasior[5], W. Gromelski[5], A. Hakola[8], X. Jiang[9], I. Jõgi[7], J. Karhunen[6], M. Kubkowska[5], M. Laan[7], G. Maddaluno[2], A. Marín-Roldán[4], P. Paris[7], K. Piip[7], M. Pisarčík[4], G. Sergienko[9], M. Veis[4], P. Veis[4], S. Brezinsek[9] and the EUROfusion WP PFC team[10]

[1] DIFFER, De Zaale 20, NL-5612 AJ Eindhoven, Netherlands
[2] ENEA, Italian National Agency for New Technologies, Via Enrico Fermi, 45, 00040, Frascati, Italy
[3] Institute of Solid State Physics, University of Latvia, Ķengaraga iela 8, Rīga LV-1063, Latvia
[4] DEP, FMPI, Comenius University, Mlynská dolina F2, 842 48 Bratislava, Slovakia
[5] IPPLM Institute of Plasma Physics and Laser Microfusion, Hery Street 23, 01-497, Warsaw, Poland
[6] Aalto University, Dept. of Applied Physics, P.O. Box 11100, 00076 Aalto, Finland
[7] Institute of Physics, University of Tartu, W. Ostwaldi 1, 50411, Tartu, Estonia
[8] VTT, P.O. Box 1000, 02044 VTT, Finland
[9] Forschungszentrum Jülich GmbH, Institut für Energie- und Klimaforschung – Plasmaphysik, 52425 Jülich, Germany
[10] www.euro-fusionscipub.org/PFC

E-mail: h.j.vandermeiden@differ.nl

Received xxxxxx
Accepted for publication xxxxxx
Published xxxxxx

Abstract

Laser-Induced Breakdown Spectroscopy (LIBS) is one of the most promising methods for quantitative in-situ determination of fuel retention in Plasma-Facing Components (PFCs) of magnetically confined fusion devices like ITER and JET. In this article, the current state of understanding in LIBS development for fusion applications will be presented, based on a complete review of existing results and complemented with newly obtained data. The work has been performed as part of a research programme, set up in the EUROfusion Consortium, to address the main requirements for ITER: a) quantification of fuel from relevant surfaces with high sensitivity, b) the technical demonstration to perform LIBS with a remote handling system and c) accurate detection of fuel at ambient pressures relevant for ITER.

For the first goal, the elemental composition of ITER-like deposits and proxies to them, including deuterium (D) or helium (He) containing W-Be, W, W-Al and Be-O-C coatings, was successfully determined with a typical depth resolution ranging from 50 up to 250 nm per laser pulse. Deuterium was used as a substitute for tritium (T) and in the LIBS experiments deuterium surface densities below 10^{16} D/cm^2 could be measured with an accuracy of ~30%, confirming the required high sensitivity for fuel-retention investigations. The performance of different LIBS configurations was explored, comprising LIBS systems based on single pulse (pulse durations: ps - ns) and double pulse lasers with different pulse durations.

For the second goal, a remote handling application was demonstrated inside the Frascati-Tokamak-Upgrade (FTU), where a compact, remotely controlled LIBS system was mounted on a multipurpose deployer providing an in-vessel retention monitor system. During a shutdown phase, LIBS was performed at atmospheric pressure, for measuring the composition and fuel content of different area of the stainless-steel FTU first wall, and the Titanium Zirconium Molybdenum alloy (TZM) tiles of the toroidal limiter. These achievements underline the capability of a LIBS-based retention monitor, which complies with the requirements for JET and ITER operating in DT with a beryllium wall and a tungsten divertor.

Concerning the capabilities of LIBS at pressure conditions relevant for ITER, quantitative determination of the composition of PFC materials at ambient pressures up to 100 mbar of N_2, the D content could be determined with an accuracy of 25%, while for atmospheric pressure conditions, an accuracy of about 50% was found when using single-pulse lasers. To improve the LIBS performance in atmospheric pressure conditions, a novel approach is proposed for quantitative determination of the retained T and the D/T ratio. This scenario is based on measuring the LIBS plume emission at two different time delays after each laser pulse. On virtue of application of a double pulse LIBS system, for LIBS application at N_2 atmospheric pressure the distinguishability of the spectra from H isotopes could be significantly improved, but further systematic research is required.

Keywords: LIBS, retention, deuterium, tritium, fusion

 © xxxx IOP Publishing Ltd

1. Introduction

Safe and successful operation of ITER requires accurate determination of the amount of plasma fuel retained in the beryllium (Be) and tungsten (W) PFCs and their deposits. In the case of Be PFCs, the majority of fuel is stored in Be deposits as found in JET [1]. During ITER shutdown phases e.g., for maintenance, the ITER vessel will be under inert gas or nitrogen just below atmospheric pressure and permit usage of remote handling systems to identify locations of deposits. Laser-Induced Breakdown Spectroscopy (LIBS) can be applied in ITER on a remote handling system to identify the location of co-deposits in the vessel as well as to determine their Tritium (T) content [2, 3]. Information of the latter is required for the nuclear safety and the estimation of the tritium inventory in the vessel. Moreover, the effectiveness of fuel removal activities like baking, Glow Discharge Cleaning (GDC) or Ion Cyclotron Wall Conditioning (ICWC) can be assessed by the LIBS system by application after wall cleaning. Most of the LIBS development work for fusion reactors in Europe is channelled through the EUROfusion Consortium where the research programme has the following main goals: a) quantification (and detailed investigations) of fuel release from W, Be and mixed W-Be deposits with LIBS, with deposits being the main retention source in ITER and b) the technological aspects of a remote handling application of LIBS inside a fusion reactor with tungsten first wall and neutrons.

LIBS [2] is one of the few available methods for quantitative in-situ determination of fuel retention in PFCs of magnetically confined fusion devices with up to 30 % operational accuracy.

In LIBS, a very small amount of material (µg) is ablated from the surface by a short (ns-ps) laser pulse, resulting in the formation of a plasma plume. Depth-resolved information on the composition of the surface layer can be obtained by recording LIBS spectra after multiple successive laser pulses at the same spatial location with characteristic ablation rate for the material. The calibration-free LIBS (CF-LIBS) method [4] is used to quantify the sample composition. The analysis is essentially based on using Boltzmann plots to extract the electron temperature (T_e) and density of each element in the LIBS plasma [5] by assuming (near) thermal equilibrium. In addition, the volume of the LIBS craters as well as the overall material density should be known for obtaining the absolute amounts of each element ablated from the surface.

Different European universities and institutes [6] joined the research for developing a LIBS system that is qualified for quantitative determination of the composition and fuel content of plasma-facing components (PFC). For validation of the LIBS approach, samples from multiple devices have been analysed by LIBS and compared with results from other laboratory techniques. For this purpose, coatings that mimic the deposits, which are expected to be formed on the PFCs in ITER (Al was used as proxy for Be), have been produced [7, 8] by laboratory experiments, either with a pre-determined concentration of plasma fuel (D or He) or with a fuel profile resulting from plasma loading in the linear plasma devices Magnum-PSI and PSI-2.

For the ultimate benchmarking of CF-LIBS application for ITER, Be-deposits themselves are indispensable, which are produced with D or He content included [9]. CF-LIBS measurements were carried out in the Be compatible facilities at the VTT Technical Research Centre of Finland. In addition, wall components from magnetically confined fusion devices (ASDEX Upgrade, W7-X and JET) have been analysed with LIBS [10, 11, 12, 13].

A remote handling application of LIBS was implemented in the FTU tokamak to demonstrate the monitoring capabilities of such a system and to allow LIBS measurements and analyses on large areas of the first wall of FTU. A compact remotely controlled LIBS diagnostic could be installed on the remote handling arm of FTU and, it proved to be a reliable tool for monitoring the composition of PFC materials inside fusion devices, within shutdown periods.

In this work the current state of LIBS development for fusion applications is presented, which is mainly based on the publications of the authors of this paper during the past four years. The main research outcomes are presented and conclusions are drawn to lay the foundations for future studies in the field. In section 2 the LIBS principle is explained and the used instrumentation is described, followed by section 3 describing the sample production as well as a motivation of the choices made concerning sample composition. In the same section the reference methods for composition determination are described. The most important LIBS parameters for quantified determination of material composition are treated in section 4, as well as the impact of external conditions on the LIBS performance. In section 5 it is demonstrated that accurate quantitative determination of the composition and fuel content of surface layers is feasible, but that there are limits in the performance at atmospheric pressure. Potential solutions to improve the LIBS performance are presented in section 6. The remote handling application of LIBS in FTU is presented in section 7. Finally, in section 8 the overarching conclusions are given together with the perspectives for applying a remote handling LIBS system in fusion technology. Moreover, in the same section a new detection scenario is proposed for enabling quantitative detection of T at atmospheric background pressures.

2. Features of applied LIBS systems

In the experiments reported here, a typical LIBS setup consists of a single-pulse (SP) or double-pulse (DP) Nd:YAG laser (see Fig. 1). The pulse width of the applied lasers was either in the ns range (laser fluence 5-65 J/cm^2) or in the ps range (laser fluence 2 - 10 J/cm^2). A spectrometer (VUV to NIR range) and/or a wide spectral range Mechelle

 © xxxx IOP Publishing Ltd

spectrometers were used for the detection of the light emitted by the LIBS plume.

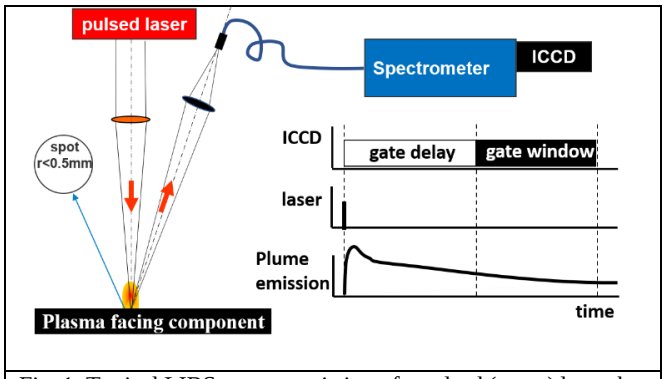

Fig. 1: Typical LIBS setup consisting of a pulsed (ns-ps) laser that is focussed on the sample and spectrometer for gated observation of the light from the laser induced plasma plume.

In the beginning of a laser pulse, during the plasma breakdown, the electron density (n_e) of the plume is very high, up to 10^{22} m^{-3}, and a significant part of laser energy will be absorbed due to inversed bremsstrahlung, reducing the amount of the laser energy available for ablation. At this phase, the emitted light cannot be used for spectral analyzes, because of the intense continuum background and the extreme Stark broadening, which limits distinguishability of the spectral lines. Depending on the ambient pressure, the plasma plume will expand with a certain rate, leading to the decay of density and adiabatic plasma cooling. At a certain timepoint of the expansion the plasma will reach thermal equilibrium and in addition, Stark broadening will be reduced. This stage is appropriate for measuring the population of the different internal states of the species enabling the determination of T_e and relative concentrations of the different species by means of Boltzmann plots. These processes have been recently characterized in detail in [14]. By utilizing a gateable detector like an ICCD (CCD camera equipped with image intensifier) corresponding spectra can be recorded by inserting a delay (typically 100 – 1000 ns) between the laser pulse and the gate window of the detector. Typical LIBS measurements are made in the range of ultraviolet (UV) to near infrared spectral range. Extending this range down to the vacuum ultraviolet (VUV) range offers the advantage that three degrees of ionization, e.g., W I-III can be measured. This allows to evaluate T_e more precisely. This advantage holds for low pressure conditions, and for oxygen-free ambient atmospheric pressure. Oxygen absorbs the emitted UV light, i.e., in that case only excited neutrals and singly ionized states would be detectable.

In order to develop a reliable LIBS system for quantitative composition measurements different laser systems were deployed and are given together with their main features:

- Single pulse LIBS (SP-LIBS): nanosecond pulse laser, pulse duration 5-12 ns, typical laser fluence 5-15 J/cm^2
- Single pulse picosecond LIBS (ps-LIBS): picosecond pulse laser, pulse duration 35-150 ps, typical laser fluence 2-10 J/cm^2
- Double Pulse LIBS (DP-LIBS): nanosecond pulse laser, pulse duration 8-12 ns, typical laser fluence 5-65 J/cm^2, typical interpulse delay less than 100 ns in vacuum to several µs in atmospheric conditions

3. LIBS test samples and their characterization

ITER-like deposits and proxies to them were used as test samples to determine the applicability of the LIBS method for quantitative material composition measurements in fusion reactors. To this end, W, W-Al, W-Be and Be-O-C coatings containing deuterium (D) or helium (He) uniformly distributed in the film matrix were produced. The W-based coatings were used, with D or He included during coating production or loaded during plasma exposure in linear plasma generators. In the Be-mixed coatings [15] D was included during production.

Beryllium is the current choice for plasma-facing material (PFM) at the first wall of ITER [16] while it will have a full tungsten divertor. The main advantages of Be are its good compatibility with the fusion plasma due to its low charge and mass (Z = 4), relatively high melting temperature (1287 °C), and the ability to getter oxygen [17]. The toxicity of Be complicates the experiments with Be coatings, and Al proxies (Z = 13), with melting point of 660 °C, are therefore commonly used as proxies to optimize the method as such. But, as a final test and necessary benchmark, Be-containing samples were analyzed by LIBS.

The fuel levels in the as-produced Be-containing samples have generally been high, from 5 up to 40 at.%, and the material structure can deviate from that of the deposits formed on PFCs of fusion devices. However, mainly impurities and material defects are determining the amount of the retained fuel, assuming that the number of BeD_x bonds are suppressed [18]. In LIBS experiments combined with different reference methods, it was shown that D retention in Al containing samples was in general much lower while the ablation rate was comparable for both Al and Be containing coatings [19]. In general, inclusion of impurities and/or fuel will enhance the ablation rate. For both Al and Be the ablation rate of D-containing coatings becomes an order of magnitude higher compared to non-doped coatings and in addition, the increasing coating thickness results also in enhancement of the ablation rate [19, 20]. Although Al and Be differ in fuel retention, in terms of validation of sensitivity and accuracy of the LIBS technique, Al certainly suffices as a proxy to optimize the method though final application as reference requires always Be. Be-oxides should be also included in this research, because these will be formed at the surface of PFCs, partly because produced PFCs contain already impurities as oxygen which are introduced during production. Moreover, oxidation of the Be surfaces inherently occurs during shutdowns of the fusion device.

All the samples investigated by LIBS have been characterized by a number of standard surface analysis methods to obtain a second opinion on their composition as well as the fuel retention. These tools include the Ion Beam

Analysis (IBA) methods Rutherford Backscattering Spectrometry (RBS), Nuclear Reaction Analysis (NRA), Secondary Ion Mass Spectroscopy (SIMS), and (Time-of-Flight) Elastic Recoil Detection Analysis ((TOF-)ERDA) as well as Thermal Desorption Spectrometry (TDS), and Glow-Discharge Optical Emission Spectroscopy (GDOES).

4. Optimization of LIBS parameters for quantifying material composition

In order to realize a reliable LIBS system for quantitative determination of the composition of investigated materials, several physics or engineering parameters need to be optimized. Moreover, the fact that LIBS has to operate during ITER shutdown phases within the vessel at atmospheric pressure, sets a challenge for the design of the LIBS diagnostic. In this section, the most important LIBS parameters will be described and if appropriate the impact of ambient conditions will be reported. In section 6 potential solutions to cope with the challenges will be presented.

4.1 Separation of H isotopes

For accurate separation of hydrogen isotope lines, the linewidths of the H isotope lines should be narrower than the difference between H_α and D_α lines (0.18 nm) or between D_α and T_α lines (0.06 nm). Typically for LIBS, the linewidth of H isotopes is determined by the Stark broadening which is related to n_e in the created plasma plume.

For LIBS at atmospheric pressures, a requirement for ITER application, the ambient gas has strong influence on both the n_e and the intensities of the H isotope lines. The use of air or an N_2 atmosphere results in fast decrease of the line intensities, which decrease to the noise level before the H isotope lines can be reliably distinguished [21]. SP-LIBS measurements showed that the line intensities decrease more slowly in an Ar atmosphere [21], allowing to distinguish the D_α and H_α lines [22]. Preliminary results show that the use of He atmospheric pressure allows to obtain the highest intensities at comparable linewidth values. Moreover, at very long detection delays, the D and H lines (even D and T) are distinguishable at atmospheric pressures, although at the costs of signal yield. The latter can be compensated by enhancing the system sensitivity on virtue of the application of large etendue optics. The measured D/H ratio (or D/T ratio) can be used for CF-LIBS (at thermal equilibrium conditions: short detection delay) for measuring the quantitative amount of fuel retained on the surface (see section 8).

The optimum ambient pressure range in terms of the plume brightness and low Stark broadening (i.e., distinguishability of the spectral lines of the H isotopes) has been noticed to be ~10 mbar, while the applied detection delays were in the 400 nm range. To cope with the variety of circumstances wherein LIBS is applied, for instance application at elevated pressure, current LIBS systems use detector schemes utilized with a gated detector to ensure the detection of light in the afterglow of the LIBS plasma where Stark broadening is diminished to the level where H isotope lines could be distinguished from each other.

In summary, using SP-LIBS H isotope lines can be distinguished at low pressures, but at atmospheric pressure, specifically in air, and as will be shown also in section 5, this is challenging and more research is required. In section 6 it will be shown that DP-LIBS can be deployed to cope with this issue.

4.2 Line intensity and sensitivity of the LIBS system

As mentioned before, increasing the background pressure results in the growth of n_e which in turn increases the Stark broadening of the lines of the H isotopes. To oppose this effect longer gate delays are used which reduce Stark broadening, but also the LIBS signal intensities. Thus, the measurement will be a compromise between obtaining narrow spectral lines and maintaining sufficient signal level.

However, the ultimate goal of this work is to realize a LIBS application on a remote handling arm. The small focal lengths involved will allow for application of large etendue detection techniques that enables to realize highly sensitive detection systems. Some examples of such high etendue systems will be presented in section 6.2.

In general, the in-situ LIBS measurements in linear plasma devices have shown improved D detection sensitivities when compared to ex-situ LIBS measurements due to reduced interference by the H_α line. This H contribution, which is normally measured during ex-situ LIBS measurements, can be attributed to water vapour deposited on the sample during air exposure before insertion in a vacuum environment.

In terms of accuracy, the signal-to-noise ratio of the spectra is important for state population measurements of the different species and therefore T_e determination. Moreover, the errors in the quantitative composition analysis depend on the uncertainties in the T_e and n_e and the fulfilment of local thermal equilibrium (LTE) for the LIBS plasma [23], thus this condition and the selected spectral lines for obtaining the Boltzmann plots have to be checked for opacity. The importance of the accuracy of T_e for CF-LIBS will be described in section 6.3.

4.3 Determination of absolute composition in PFCs

As stated in [2] the most important research task is the conversion of the LIBS signal into relative composition of the material including the fuel content and finally the absolute composition of the deposited wall material.

The features of the CF-LIBS method are described in the previous sections, and it provides the relative elemental composition of the studied materials. An alternative more empirical method is the so-called slope-ratio method [24]. Also with this method, the relative composition and fuel retention of wall materials can be determined by making use of an experimental database containing ablation characteristics from multiple pure bulk materials. The method is based on the assumption that for a particular LIBS setup and

irradiation conditions, the signal intensities (accumulated signal per laser shot) from pure bulk material (from database: ex-situ experiments) can be compared with signal intensities from the material to be investigated, giving the relative amount of that element in the material. The surface morphology is not included in this method, but experiments show no large deviations [24]. However, in case the T_e (determines excitation energy of the elements) in the plasma plume for the reference bulk sample differs from that of the unknown layer (due to mixed material, morphology effects, or laser impact variation) deviations can be expected [2, 24]. This necessitates reference measurements with samples mimicking ITER-relevant mixed layers. However, in combination with this empirical method, CF-LIBS can be used to determine the T_e parameter accurately, which mitigates this disadvantage. Nevertheless, because the CF-LIBS is far more developed and straightforward, it was decided to use CF-LIBS for determination of the relative composition of the materials to be investigated. For absolute determination of the composition and fuel content of a priori unknown material CF-LIBS (and/or slope-ratio method) can be used. In case the bulk density of the material to be investigated is approximately known, the results from CF-LIBS can be combined to obtain the quantified amount of ablated material in the plasma plume, thus the error bars will depend mainly on the accuracy in the bulk density estimation.

Another obvious method is to use directly the absolute photon efficiencies of LIBS (ablated atoms per number of emitted photons) for each element. Together with the known detection solid angle (and ablation area) and transmission of the LIBS detector system the absolute amounts of the elements in the material surface can be determined.

An overarching requirement in this work is that stoichiometric ablation as well as good correspondence between amount of ablated material and plume content can be assumed [25]. In respect to this the formation of droplets during laser-material interaction could cause deviations, because these are not detected directly by the LIBS observation system. The droplets are formed after the plasma formation [26] and it is expected that gas desorbed from these droplets can only very minorly affect CF-LIBS results.

5. Demonstration of quantitative D retention measurements of ITER-relevant coatings

In this section we review how LIBS can be deployed for quantitative determination of material composition and fuel content of fusion-relevant samples. The results have been extracted from experiments where LIBS was performed at background pressures from a few mbar up to around 1 atm. Other parameters varied in the measurements were the sample type, laser fluence, width and delay of the recording gate. It should be noted, that quantitative D composition analysis by CF-LIBS was only applied for LIBS based on ns lasers.

The following samples were used: coatings on a Mo substrate like W-Al-D (~5% D), but also Be-containing coatings comprising W-Be-D (~5% D) and furthermore on a W substrate: Be-D (~20% D), Be-O-D (~25% D) and Be-O-C-D (~41% D).

5.1. SP-LIBS for determination of D retention in Be-mixed coatings at low pressure

For W-Be-D and Be-D coatings, the studies were conducted at low pressures (≤10 mbar). Coatings containing Be-D, without W, were used for LIBS studies at ambient pressures from 1 to 10 mbar [15], and for W-Be-D coatings LIBS was carried out at a 0.5 mbar Ar pressure [19, 27], which measurements are shown in Fig. 2 and Fig. 3. Fig. 2 [19] shows the decaying tendency of D_α and H_α spectral lines for the first 10 laser shots. The D content was determined by CF-LIBS after fitting the combination of the H_α/D_α spectral lines as is demonstrated in Fig. 3. The average value over the entire layer thickness (2 µm) was found to be 5.9±3.3 % (5×10^{17} D/cm^2) [27] (ablation rate 275 nm/shot), and was in good agreement with TDS results [27].

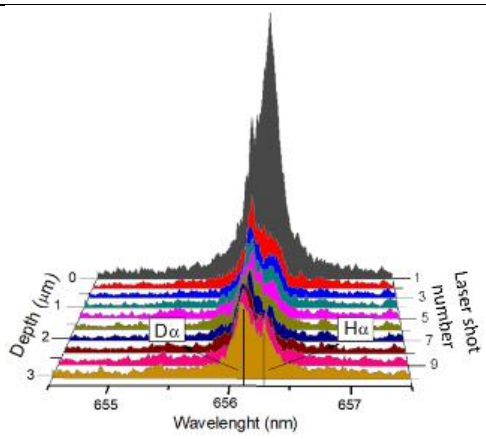

Fig. 2: LIBS spectrum from 10 laser shots, the first shot gives the highest H/D level and drops for increasing penetration [19]. SP-LIBS: ablation rate 275 nm/shot, P = 0.5 mbar Ar, delay time 150 ns. Material: W-Be-D coating on a Mo substrate.

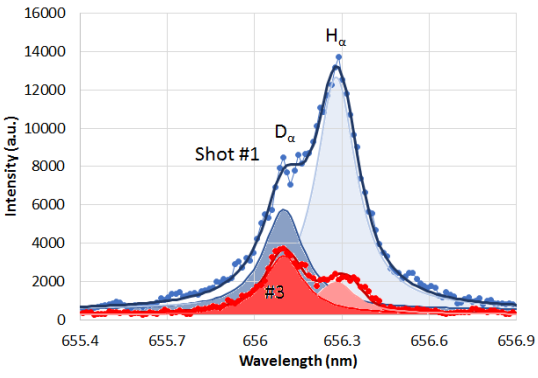

Fig. 3: LIBS spectrum corresponding to shot numbers: 1st and 3rd laser shot shown. D content $5 \cdot 10^{17}$ D/cm^2 [27]. SP-LIBS: 4.5 J/cm^2, ablation rate 275 nm/shot, P = 0.5 mbar Ar, delay time 150 ns. Material: W-Be-D coating on a Mo substrate. The W 653.3 nm line was included in the fitting of the D and H peaks, but is for clarity omitted in Fig. 3.

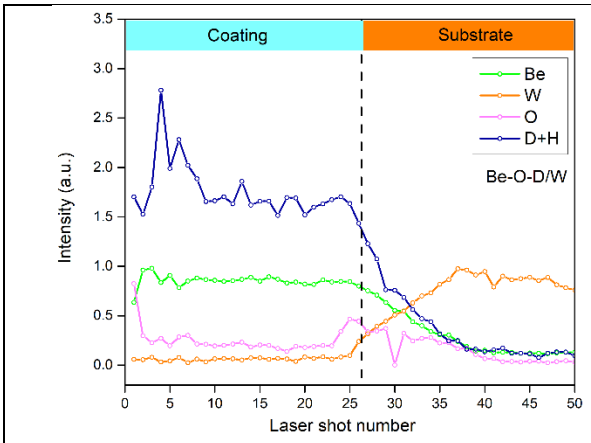

Fig. 4: LIBS depth profiles, showing the limit of the coating at the laser shot number 26 [15].
SP-LIBS: fluence 4.5 J/cm^2, ablation rate 230 nm/shot, P = 10 mbar Ar, delay time 150 ns. Material: Be-O-D coating on a W substrate.

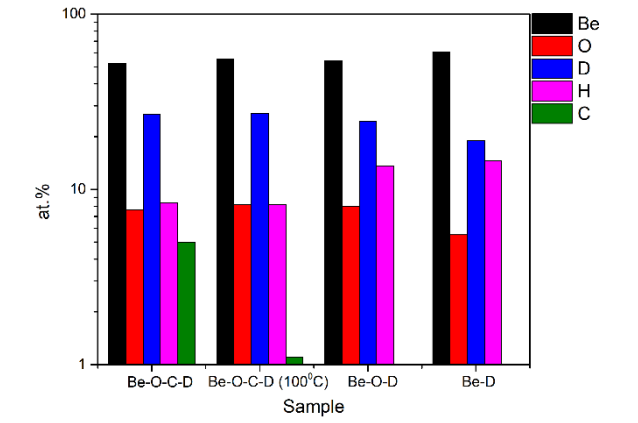

Fig. 5: Relative elemental composition determined by CF-LIBS of the whole deposited layer for four different samples [15].
SP-LIBS: fluence 4.5 J/cm^2, ablation rate 230-360 nm/shot, P = 1 - 10 mbar Ar, delay time 150 ns. Material: Be-mixed coatings (i.e., Be-O-C-D, Be-O-D, and Be-D) on W substrates.

In Fig. 4 the LIBS depth profiles of elemental composition of a more sophisticated Be-O-D (including H) sample, measured at 10 mbar Ar pressure, are presented [15]. For four different samples, the elemental composition averaged over the deposited layer (26 laser shots for Be-O-D sample) is summarized in Fig. 5. The results were in good agreement with the results of IBA.

5.2. SP-LIBS for determination of D retention in W based coatings at pressures up to 1 bar

SP-LIBS was applied at 100 mbar N_2 pressure, to perform CF-LIBS analysis on W-Al-D samples (thickness 3 µm) [23]. The measured D content 4±2% (**4×10^{17}** D/cm^2**,** average ablation rate 250 nm/shot) corresponded within 25% with the values found with GDOES. The high H content limited the D detection sensitivity to 2×10^{17} D/cm^2, i.e., at pressures close to atmospheric pressure, the Stark broadening became important and H_α peak starts to interfere with the D_α peak.

Additional CF-LIBS research for D retention measurements on W-based alloys was carried out at 1 bar ambient pressure, using both air and N_2 gas flows. A study with W-N-D sample [28] (N: 5-10 at.% and D: nominally 5 at. %) was performed in air atmosphere with SP-LIBS, using a delay time of 3.8 µs. At this delay, the D_α line was still detectable but not yet distinguishable from the H_α line. The intensity of the D_α line was obtained by fitting overlapping H_α and D_α lines with Voigt profiles. A D content of ~3 at.% was found with CF-LIBS, which is in reasonably agreement with the nominal value (5 at. %), although underestimated [28]. With the same setup, but this time at N_2 atmospheric pressure, another LIBS study was performed using a W/Ta (Ta: 5 at. %) sample, containing a nominal D content of 5 at. % (coating thickness ~3 µm) on a Mo substrate. With the adopted experimental parameters, it was not possible to perform CF-LIBS because of the strong overlap of the Ta I line at 656.15 nm with the D_α line and further tests are scheduled, using different background gases or by applying a partial vacuum to circumvent this issue [28].

In another experiment, a W-Ta sample (Ta: 5 at. %, nominal D content of 10 at. % (coating thickness ~3 µm)) was investigated with CF-LIBS at both air and N_2 atmospheric pressure [29]. The Ta emission lines have been used for CF-LIBS analysis to determine T_e, (measurement delay 1µs for both background conditions). In both cases, the LIBS spectra exhibited a significant interference between the Ta I line at 656.15 nm and the D_α line at 656.1 nm, which limited satisfactorily discrimination of these lines. A numerical profile simulation was used to calculate and subtract the intensity of interfering H_α (656.28 nm) and Ta I (656.15 nm) lines, and a D content of 20 at.% was found [29]. In these experiments the CF-LIBS showed an overestimation of the D content by more than 50%.

To improve the measurement accuracy the application of a background gas consisting of lower mass species (He) or a local vacuum by means of a separate cylinder can mitigate the limitations caused by the Stark broadening of the Balmer-α lines of hydrogen [28].

Summarizing, from the results of SP-LIBS experiments described above it can be concluded that CF-LIBS is performing accurately at ambient pressures up to 100 mbar N_2, also the D_α and H_α lines were well distinguishable and these results were within 30% in agreement with IBA measurements. At atmospheric pressure, the measurement accuracy of CF-LIBS decreases and further research is required. A viable direction to overcome the issues in terms of sensitivity and distinguishability of these lines is the application of a LIBS detection scheme as proposed in section 8, but first in section 6 some more established methods for improvement of the LIBS performance are described.

6. Enhancing LIBS performance

As mentioned in subsection 4.1 and also shown in section 5, LIBS operation at atmospheric pressures is demanding, and therefore, different signal enhancement techniques have been investigated in terms of plume brightness, SNR, SBR and sensitivity.

6.1 Intensity and distinguishability of spectral lines

The lifetime of a LIBS plasma plume is short, typically 100 ns in vacuum and ~5 μs at atmospheric pressure. Concentrations of H-isotopes are normally measured with a certain delay after the laser pulse in the afterglow of the plasma plume, i.e., then the Stark broadening of the spectral lines as well as the emission strength is reduced [22]. The prolongation of the laser-induced plasma lifetime can solve these problems and two main LIBS schemes were successfully explored using a second laser pulse or alternatively a spark discharge for the re-excitation of the LIBS plasma in the afterglow [30, 31]. Prolongation of the lifetime allows obtaining lower n_e due to the plasma expansion, while T_e remains at comparable values as in the initial plasma. In this way, the separation of the H_α and D_α lines become possible even at atmospheric pressures [21], and enables quantitative retention measurements with CF-LIBS. The enhancement of emission and plasma lifetime can be obtained, for example, by re-excitation of the initial LIBS plasma, by a second laser pulse (DP-LIBS), which enhances the plume emission by a factor ~4 [30].

Regarding DP LIBS, the first laser pulse is followed by a second one, which is delayed with a time scale shorter than laser-target interactions. Plasma confinement in the low-pressure gas volume induced in front of the target after the first laser pulse is thought to play a significant role [32], i.e., the plasma produced by the first pulse expands, and pushes out the ambient air near the target and thus produces for a certain time a low-pressure zone in which the second pulse can interact. This is the reason why the intensity of the spectral lines originating from the ambient gas significantly decreases in the second pulse, i.e., at this phase invasion of the induced zone by particles from the ambient gas is temporarily avoided. Due to long plasma lifetime, the gases desorbed from the interaction area have some time to enter the high-temperature area to get excited and to emit light. The difference in performance is demonstrated by comparing DP-LIBS and SP-LIBS on a D loaded W-Al-D coating on a Mo substrate. This newly obtained data, extracted from [33], and plotted in Fig. 6 demonstrates that for DP-LIBS, the signal-to-noise ratio together with the dynamic range are much higher and the measurement uncertainties are much smaller relative to those obtained with SP-LIBS. Moreover, the Stark broadening effect may be substantially reduced with the use of DP LIBS, because it allows for the decrease of n_e of even a factor 4 [34], and in general this is accompanied with the improvement in signal quality [30]. This performance was tested and confirmed by DP LIBS measurements at atmospheric pressures [33].

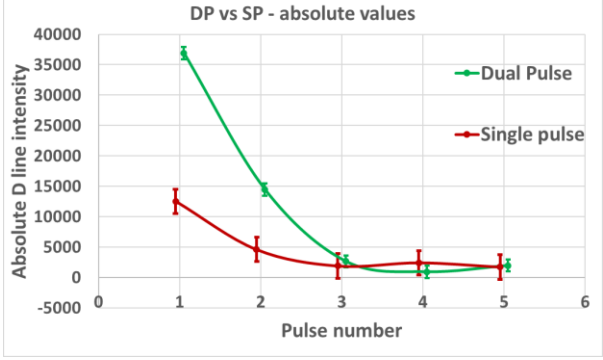

Fig. 6: D signal intensity for subsequent pulses in DP and SP LIBS performed at a D doped coating. Note that for DP the signal is higher and the error bars are smaller. The latter due to improved contrast relative to the spectral lines originated from the background particle emission. For both LIBS measurements the parameters were the same: ablation rate 250-300 nm/shot, P = 10^{-2} mbar air. Material: W-Al-D coating

As mentioned before, for elemental quantification by CF-LIBS, a precise T_e determination is crucial. Fortunately, W has a large number of suitable lines (this is not the case for Be, C, O, etc.) for making accurate Boltzmann plots. The improvement of T_e determination could be obtained by using all three degrees of ionisation, W I-III, by including also the VUV spectral range [35].

6.2 System sensitivity

In section 4.2 it was mentioned that the application of LIBS on a remote handling arm, has advantages in terms of etendue enhancement of the detector system, because of the short observation distance of the LIBS plume. This was demonstrated by an LIBS experiment carried out at the linear plasma device PSI-2 [36]. The dynamic retention (outgassing) from W samples was determined in the linear plasma device PSI-2, wherein W samples were exposed by D plasma [37, 38]. The outgassing was investigated *in situ* by SP-LIBS (532 nm, 8 ns, 40 J/cm^2) in vacuum. The correspondence of LIBS D_a line intensity to D content in the D plasma exposed W sample was calibrated by TDS and NRA. The detection limit of the LIBS system was about 10^{15} D/cm^2 on virtue of a Littrow spectrometer with a large etendue of 2.4×10^{-4} cm^2 srad. Within ~200 min after plasma switch-off, D retention was reduced with a factor of 3-6 (depending on the radial position of the laser spot on the sample), and stabilised to a level of about 5×10^{16} D/cm^2 (probing depth 200 nm) (see Fig. 7 and 8) [37, 38].

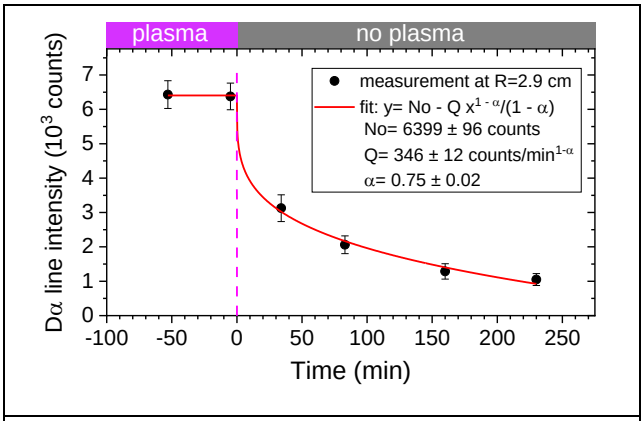

Fig. 7: LIBS signal of D_α line measured directly after plasma exposure in PSI-2. Fit assumes that outgassing decay follows a single power law with exponent α. SP-LIBS: ablation rate ≈200 nm/shot, P = 10^{-7} - 10^{-4} mbar D_2, Material: W sample.

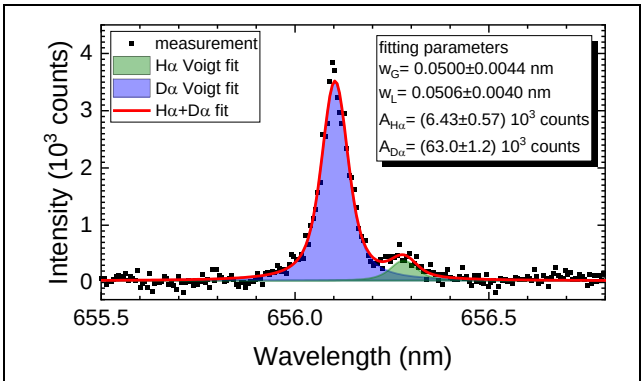

Fig. 8: LIBS spectrum corresponding to one of the data points shown in Fig. 7 [37].

Similar outgassing experiments were carried out with SP-LIBS (at 1 mbar Ar pressure) in Magnum-PSI [39]. Two hours after (D) plasma switch-off LIBS measurements could be performed. The results together with complementary in-situ NRA measurements demonstrated negligible D outgassing between 2 to 42 hours after plasma switch-off stabilizing to D retention values of 1-6×10^{16} D/cm^2 (probing depth 1 µm), depending on position along the sample and coating type (porous or compact W coatings).

6.3 Determination of T_e in plasma plume

For improving the accuracy in the T_e evaluation, a ps laser instead of a ns laser can be used for LIBS [40]. However, to obtain a sufficiently high D/W ratio for D_α and the strongest W I line at 400.8 nm, T_e should not to be lower than approximately 0.7 eV, according to the LIBS web spectra simulations [41]. The necessity of a precise T_e determination is presented in Fig. 9, showing the dependence of the calculated elemental composition in a Be-D sample as a function of T_e: 0.1 eV uncertainty of T_e causes a difference of 27.5% in the calculated D content [15].

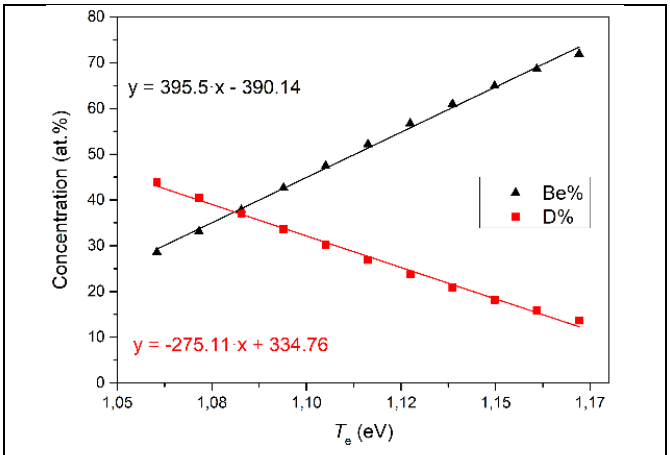

Fig. 9: Variation of CF-LIBS results: calculated relative elemental composition (at.%), for varying T_e [15]. The uncertainty in the T_e evaluation leads to an error in the concentration calculation, which shows the importance of correct T_e determination.

6.4 Ablation characteristics: comparison ps-ns based LIBS systems and depth profiling

The type of lasers used for LIBS determines in general the ablation characteristics. Craters formed due to ablation by lasers with nanosecond pulse duration are characterized by local melting due to heating effects. This effect is more pronounced for metallic materials [42], and could lead to inaccuracy of the fuel measurement in multi pulse LIBS, due to enhanced diffusion of the fuel particles from the hot near-surface layer between the laser pulses. The latter will reduce the amount of detected fuel particles for the following laser pulses. The effect strongly depends on the heat penetration, which is defined by the power density in the laser spot. When this exceeds a critical value, a shockwave will form and propagate until a certain depth through the bulk target. The significance of this effect for LIBS is still under discussion.

Conversely, lasers exhibiting picosecond pulse duration enable crater formation with near ideal ablation, i.e., without significant melting effects [43]. It is worth noting that the duration of the (ns) laser emission that reaches the target surface is shorter than the laser pulse duration itself due to plasma shielding after plasma breakdown. The increase of the power density in the laser spot reduces the duration of the laser-material interaction. This effect is most pronounced for long wavelength laser radiation and high ambient gas pressure.

Experimentally, the effect of laser-pulse duration was investigated by LIBS measurements using lasers with pulse widths of 150 ps and 8 ns, respectively, for ITER-relevant samples [44]. The elemental depth profiles of the samples with W-Al-D coatings (thickness 3 µm, 10 at.% of Al, 5 at.% of D) on Mo substrates are illustrated in Fig. 10 and Fig. 11. Both lasers were operated at 1064 nm, whereas the laser fluence at the target for nanosecond and for picosecond lasers were 10.6 J cm^{-2} and 5.5 J cm^{-2}, respectively. Considering the thickness of the coating determined by GDOES, the estimated ablation rates were 290 nm/shot and 170 nm/shot, showing that the

ablation rate for ps-lasers was much lower than that for ns-lasers.

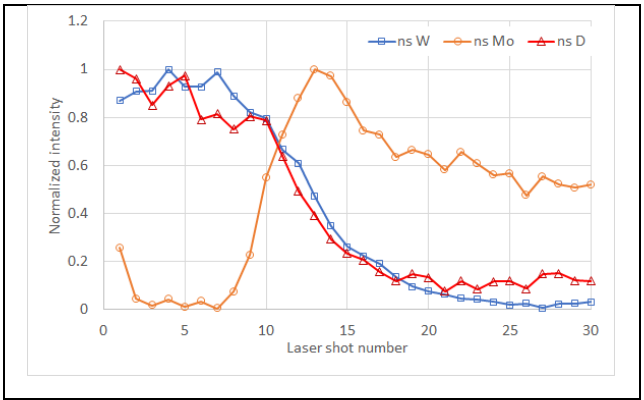

Fig. 10 Elemental LIBS depth profiles by a ns pulse laser. Coating 3 μm, 10 at% Al, 5 at% D on Mo substrate [44]. (fluence 10.6 J/cm^2). This performance should be compared with the results obtained with a ps laser (Fig. 11).

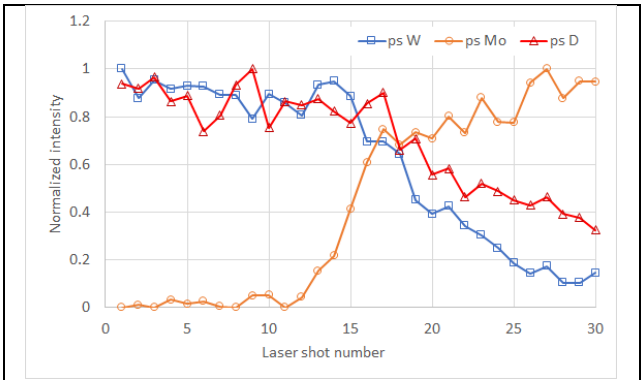

Fig. 11 Elemental LIBS depth profiles by a ps pulse laser. Coating 3 μm, 10 at% Al, 5 at% D on Mo substrate [44]. (fluence 5.5 J/cm^2).

A lower ablation rate, as expected for ps-LIBS, can lead to lower brightness of the LIBS plume. However, as mentioned before, large solid angle detection optics can be used to compensate for this. In the following the performance of a ps-LIBS system is described, where it was shown that ablation rates even down to 30 nm/pulse are not an issue.

At a pressure of $2{\cdot}10^{-7}$ mbar, ps-LIBS was applied for composition analysis of divertor baffle screws [12] and for erosion/deposition mapping of W7-X divertor tiles [13]. The graphite tiles have a Mo marker interlayer with a thickness of 0.2–0.4 μm, which is covered by a 5–10 μm thick carbon layer. The number of laser pulses (λ=355 nm, 2.3 J cm^{-2}, 35 ps) was applied at each probing location to perform the depth profiling by using Mo line emission (see Fig. 12). The ablation rates in regimes 1, 2 and 3 were found to be 108±0.5 nm/pulse, 44±2.8 nm/pulse and 30±3.8 nm/pulse, respectively.

The same LIBS set-up was used for depth profiling of a Mo sample with a 4.6 μm W-columnar coating thickness. A Littrow spectrometer [45] with an etendue of $6.4{\times}10^{-5}$ cm^2 srad was used for the detection of the LIBS spectra. This sample was exposed to the deuterium plasma in PSI-2. The measured depth profile of D, W and Mo elements is shown in Fig.13. Only H_α line was observed in the first laser pulse and the integral line intensity was about 4.2 times that of D_α. The ablation rate of this W coating was about 16 nm/pulse providing the depth resolution approaching to that obtained by the SIMS method.

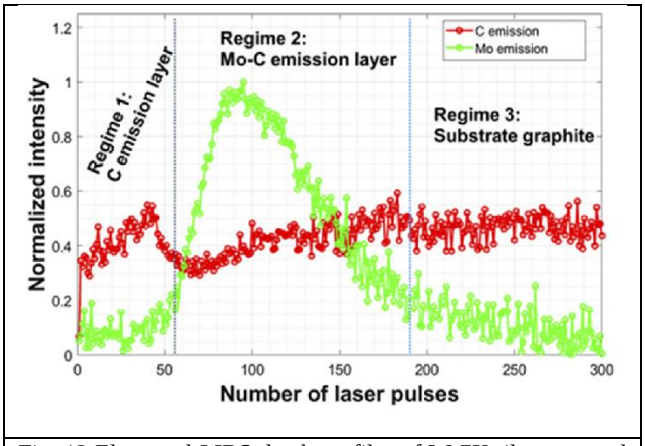

Fig. 12 Elemental LIBS depth profiles of W-7X tile measured by 35 ps laser. (λ=355 nm, fluence=2.3 J cm^{-2}) in vacuum [12].

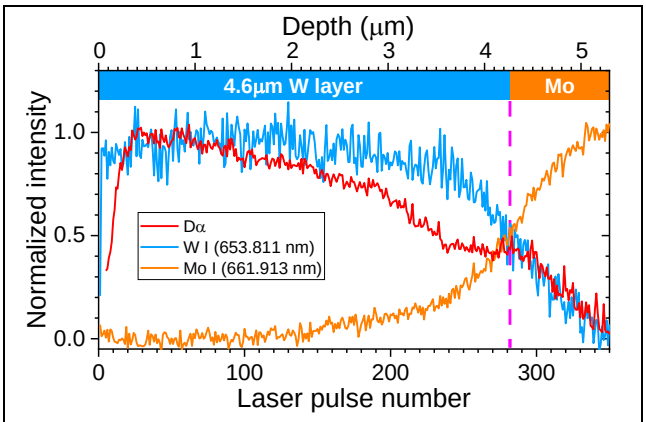

Fig. 13 Elemental LIBS depth profiles of 4.6 μm W-columnar coating on Mo substrate measured by 35 ps laser. (λ=355nm, fluence 1.7 J/cm^2) in vacuum.

The measurements presented in this section show that LIBS allows for depth profiling with a controlled resolution varying from about 15 nm up to 400 nm/shot.

7. Remote handling application of LIBS in the FTU tokamak

To allow LIBS measurements and analyses on larger areas of a first wall (FW), a compact and light LIBS tools could be installed on remote handling systems and used during shutdown and maintenance periods of fusion devices. In conjunction with the standard systems outside the vacuum vessel, such compact devices, intended as a 'plug-in' diagnostic, would ensure full time, large area monitoring of the PFCs.

Following this guideline, a compact and light DP-LIBS system (520×340×86 mm^3, weight < 10 kg) (Fig. 14) was developed and mounted on the FTU multipurpose deployer,

performing LIBS analyses on the FTU FW, after the first D retention measurements were successfully carried out from outside of the FTU toroidal limiter [46]. The system was connected with a broadband (210–800 nm) and a narrow spectral range (8-20 nm) spectrometer (fiber-based relay system) through a bifurcated optical fiber, to detect as much as possible emission lines from all the chemical elements present in the LIBS plasma and to monitor with high spectral resolution, the D_α/H_α emission lines from H and D. On virtue of a pressure confinement tube, the system allows for measuring in vacuum (>10^{-3} mbar) as well as at atmospheric pressures or under gas flows (Ar, He, N_2, etc.) [21], i.e., adapting the operating conditions for maximum sensitivity and minimizing Stark broadening.

The LIBS system enabled to investigate large areas of the FTU vacuum vessel (Fig. 15) and the main results obtained in [46] were confirmed, in particular, the ubiquitous Li contamination of the FW, ascribed to previous experiments with liquid Li limiters inside FTU [47].

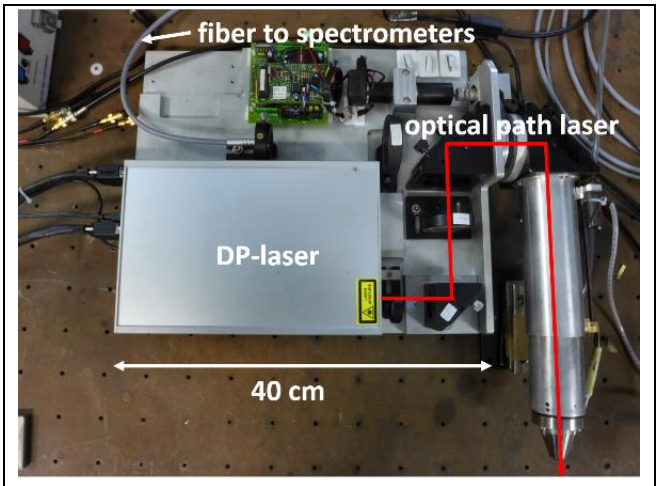

Fig.14: The compact LIBS device. Weight < 10 kg.

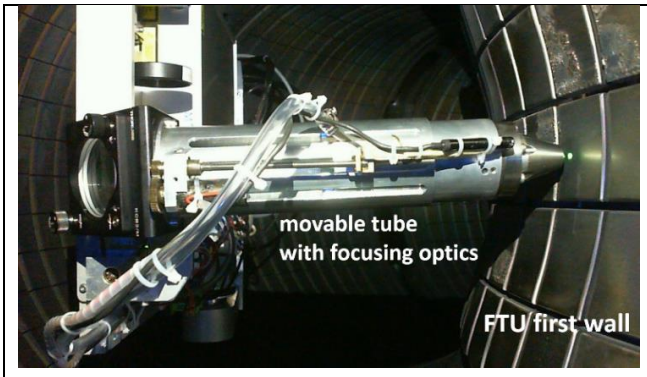

Fig. 15: LIBS device mounted on the FTU multipurpose deployer.

Then the superficial stratigraphy of the Stainless-steel grade 304 (nitrogen-strengthened) (SS 304 LN) elements of the FW, contaminated with Li, Mo, Ti was clearly detected (Fig. 16) [48], Mo and Ti being detected as erosion products of the titanium-zirconium-molybdenum (TZM) tiles of the toroidal limiter. The FW showed also a deep H contamination, clearly detected during the depth profiling analysis (Fig. 17) [48]. This behaviour is probably due to venting of FTU in between experimental campaigns and due the chemical interaction of H and D with the superficial Li [21] in the presence of air. A similar contamination by B and C was also found by CF-LIBS analysis of screws removed from the COMPASS tokamak after a Li campaign [49]. This activity demonstrated the feasibility of LIBS systems as a "plug-in", compact and light tools, to be used as a fast and reliable analytical technique to monitor large areas of the FW and divertor and different PFCs in next generation fusion devices. To our knowledge, this represents the first prototype of such system application within a fusion device.

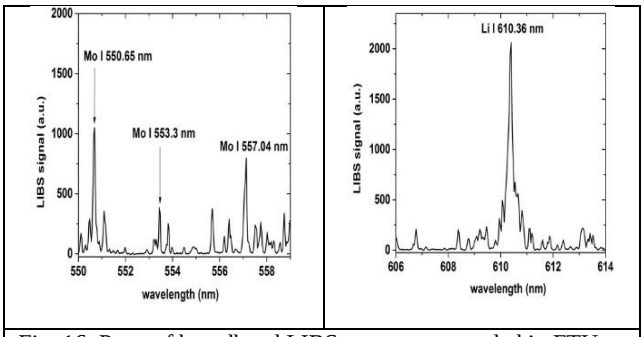

Fig. 16: Parts of broadband LIBS spectrum recorded in FTU [48].

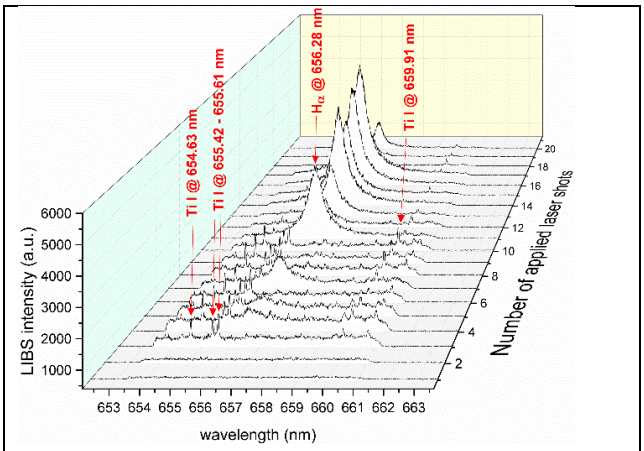

Fig. 17: High-res depth profiling analysis on a stainless-steel element of the FTU FW [48]. LIBS Measurements were carried out at *atmospheric air pressure*, laser ND:YAG (λ = 1064 nm, pulse duration 9 ns).

8. Conclusions and outlook

In this section the conclusions and outlook are presented. The main aim of this work is to optimize LIBS for quantified determination of fuel content in W, Be and mixed W-Be deposits and to show the feasibility of LIBS as a remote

handling diagnostic to monitor composition and fuel content of the surfaces of PFCs in a fusion reactor.

It should be noted that this work describes T retention measurement systems that should operate during the maintenance phase of a fusion reactor and perform measurements over a wide area inside the reactor vessel. For in-situ measurement of T during the operational phases of the reactor some LIBS systems are already designed or tested [50, 51, 52], these systems are mainly applied for a limited number of locations in the first wall of the reactor. Secondly, it is noted that the scope of this work concerns the conceptual design of a LIBS system that will be applied during maintenance periods of a fusion reactor, issues concerning neutron radiation from the activated vessel components are beyond the scope of this work. Such violent radiation environment requires special shielding measures, but possibly also silica based fibers with high radiation resistance like proposed in [53].

A summary of the obtained results is given in table 1. for the different LIBS systems applied during this research.

Table 1	
SP-LIBS	
Ablation rate /laser fluence	60-160 nm/pulse (W) 7 J/cm^2 [54] 400-800 nm/pulse (porous W-Al) 7 J/cm^2 [54] 250-500 nm/pulse (columnar W-O) 15-20 J/cm^2 [39, 55] 210 nm/pulse (W-N-D) 66 J/cm^2 [28]
Operational press. range H isotope distinguishability	1 bar N_2 or air [28] Quality: high till 100 mbar N_2 [23] At 1 bar Ar [22] Distinguishable at long delays with low S/N ratio
Highest operational press. CF-LIBS and D content accuracy	1 bar N_2 or air [29, 39] ~50%
Typical sensitivity H isotopes	>5 at.% at 1 bar pressure <0.5 at.%, in-situ LIBS @ 1 mbar [39]
DP-LIBS	
Ablation rate/ laser fluence	100-500 nm/pulse 6.5 - 25 J/cm^2 [25, 30] (W, W-Al, Mo-W-Al)
Operational press. range H isotope distinguishability	10^{-5} mbar to 1 bar air Quality: dependent on detector resolution
Highest operational press. CF-LIBS* and D content accuracy	1 bar or air [27, 33] Statistical error <10%
Typical sensitivity H isotopes	<2 at.%
ps-LIBS	
Ablation rate/ laser fluence	16 nm/pulse, 1.7 J/cm^2 (35 ps, 355 nm) (W-columnar coating) 40 nm/pulse, 5.3 J/cm^2 (35 ps, 355 nm) (W) [56] 200 nm/pulse, 12 J/cm^2 (35 ps, 355 nm) (W) [56] 500 nm/pulse, 20 J/cm^2 (35 ps, 355 nm) (W) [56] 170 nm/pulse 5.5 J/cm^2 (150 ps,1064 nm) (Mo-W-Al) [44]
Operational press. range H isotope distinguishability*	Good line separation 2×10^{-7} mbar and <5 J/cm^2 (35 ps laser, 335 nm) 3 mbar Ar at 5.5 J/cm^2 (150 ps, 1064 nm) [44]
Highest operational press. CF-LIBS*	Not applied yet
Typical sensitivity H isotopes*	4×10^{13} D/cm^2 at 16 nm/pulse at 1.7 J/cm^2 (35 ps, 355 nm)

* Not fully explored up to atmospheric pressures

From the table and the described experimental work carried out the following conclusions can be made:

1. With CF-LIBS the fuel content of the samples were obtained with an accuracy of 30% for background pressure conditions up to 100 mbar. For CF-LIBS at atmospheric pressure conditions the deviations in fuel content were above 50% and more research is required to demonstrate the applicability of CF-LIBS for quantified retention measurements at these ambient conditions.
2. CF-LIBS validation experiments carried out at low pressure have proven that accurate quantitative results with accuracies up to 30% were obtained for a variety of ITER-relevant coatings. Results from CF-LIBS investigations of W, W-Al, W-Be and Be-O-C coatings (with D or He content) were confirmed by standard surface analysis techniques.
3. D and H lines can be distinguished, even at atmospheric pressure by using DP-LIBS [28], but also by SP-LIBS with optimized timing [22].
4. Fuel retention measurements with DP-LIBS features the best performance in terms of signal-to-noise ratio and distinguishability of the lines from H isotopes.
5. The ps-LIBS system enables reaching depth resolutions down to 20 nm (see Fig. 13). This would also allow the detection of supersaturated layers (W lattice saturated with fuel) which are formed at the very surface, directly after plasma exposure. It was also shown that ps-LIBS has an advantage in comparison with ns-LIBS for the measurement of fuel content due to the smaller thermal effects and lower ablation rate. The significance of this effect for CF-LIBS needs further research. For both ns-LIBS and ps-LIBS the accuracy in absolute depth profiling, or the total penetration depth of the LIBS craters is an issue, a method to measure the absolute probing depth is required, or it should be possible to use marker material embedded in the surfaces.
6. The accuracy in quantitative composition determination is strongly affected by the accuracy in T_e [15] in the LIBS plasma plume and requires careful setting of detection delays.
7. The application of large etendue optics in remote handling LIBS systems enables fuel detection levels down to 10^{15} D/cm^2 [37, 38].

In general, it has been shown, that a careful analysis of SP-LIBS spectra at the Balmer-alpha spectral region of H isotopes allows to distinguish the spectral contributions of the H isotopes, enabling to apply the CF technique including the quantification of these H isotopes. The results show that the D content is possible to estimate, although an underestimation of 20-40% is observed compared to the given nominal content

[23, 28]. This underestimation can result from two factors: 1) hydrogen-deuterium isotope exchange, reducing the initial amount of deuterium in enriched samples after their exposure to environmental conditions with water vapour present, a factor that in real ITER PFCs and current fusion devices should be reduced in case of analyses carried out with LIBS in the reactor vessel at air ambient pressure. 2) an incomplete achievement of LTE for H isotopes.

As can be concluded from aforementioned discussions the application of CF-LIBS at atmospheric pressure conditions is most challenging in terms of sensitivity and distinguishability of D_α and H_α lines (in ITER: D_α and T_α). In order to solve these issues, the authors propose the following LIBS scheme, which is possible on virtue of the application of large etendue optics:
1. Perform for each laser pulse CF-LIBS (detection window at short time delay relative to laser; plume plasma in thermal equilibrium), in that case due to Stark broadening the D_α and T_α signal will overlap and cannot be resolved. However, it allows to obtain a D/T integral signal with a good SNR and enables quantification with CF-LIBS.
2. The second measurement can be done at long delays (in the range of microseconds), i.e. Stark broadening is minimized and D_α and T_α are distinguishable. This enables to measure the T/D ratio and this information can be used for the CF-LIBS measurement results obtained in the first detection window

For each laser pulse, the detection of the light mentioned in item 1 and 2, are subsequently performed. The difference with a standard LIBS system is that the detection is performed two times after each laser pulse instead of one time. In practice, this procedure can be carried out by using a bifurcated optical fiber combined with for instance 2 spectrometers that are both equipped an ICCD camera. One spectrometer with a large wavelength range for CF-LIBS measurements (short delays) and one large etendue spectrometer with narrow spectral range for distinguishing the isotopic lines (using long delays). This enables to measure the absolute T amount by using a single laser pulse. Moreover, the T/D ratio measured in the scrape-off layer plasma by optical emission spectroscopy diagnostics at the fusion reactor can be used for retrieving indications of the expected D/T ratio in the PFCs. However, the plasma conditions and D/T ratio will vary in the different plasma campaigns, thus uncertainties in the ratio of the retained fuel are to be expected. To determine the limits in terms of sensitivity and line distinguishability of the proposed LIBS measurement scenario further investigations are required.

Moreover, in this work an innovation was used in order to circumvent the mentioned issues encountered at atmospheric pressure conditions. A flow of shielding gas (Ar or He) was used at the LIBS spot, or LIBS measurements were performed at optimized vacuum conditions in a compact confinement cylinder as demonstrated in FTU.

Thick layers of Be containing layers are expected to be formed on PFC surfaces, the material density will vary and with this also the ablation rate, causing inaccuracies for depth profiling (see item 5 of this section). The application of a compact confocal microscope [57] could be beneficial for monitoring the ablation rate.

A remote handling application of LIBS was successfully implemented by using a robotic arm in FTU. A compact DP-LIBS system, able to pass through the narrow FTU equatorial port was mounted on the end effector of the FTU robotic arm: by combining the toroidal motion of the arm with the full poloidal rotation of the tube supporting the focusing lens, the elemental composition of any point of the vacuum vessel was tested without losing performance quality compared to an *ex-situ* analysis.

In summary, after introducing further improvements, a LIBS-based system, as proposed as T monitor in ITER, will be capable to operate under the most demanding conditions.

Acknowledgements

This work has been carried out within the framework of the EUROfusion Consortium and has received funding from the Euratom research and training programme 2014-2018 and 2019-2020 under grant agreement number 633053. The views and opinions expressed herein do not necessarily reflect those of the European Commission.

This scientific work of the authors from IPPLM was supported by Polish Ministry of Science and Higher Education within the framework of the scientific financial resources in the years 2010–2020 allocated for the realization of the international co-financed project. Comenius University authors would like to thank for partial financial support by SRDA (APVV-16-0612) and by VEGA (1/0803/21). Institute of Solid State Physics, University of Latvia, as the Centre of Excellence, has received funding from the European Union's Horizon 2020 Framework Programme H2020-WIDESPREAD-01-2016-2017-TeamingPhase2 under grant agreement No. 739508, project CAMART^2.

References

[1] Brezinsek S, *et al, J. Nucl. Mater.* **463** (2015) 11-21
[2] Philipps V, *et al. Nucl. Fusion* **53** (2013) 093002
[3] Maurya G S, *et al, J. Nucl. Mater.* **541** (2020) 152417
[4] Ciucci A, *et al*, *Appl. Spectrosc.* **53** (1999) 960
[5] Aguilera J, *et al*, *Spectrochim. Acta B* **62**, Issue 4, (2007) 378
[6] Brezinsek S, *et al, Nucl. Fusion* **57** (2017) 11604
[7] Grigore E, *et al, Nucl. Mater. Energy* **9** (2016) 137-140
[8] Dellasega D, *J. Appl. Phys.* **112** (2012) 084328
[9] Nemanic V, *et al, Fusion Eng. Des.* **150** (2020) 111365
[10] Karhunen J, *et al, J. Nucl. Mater.* **463** (2015) 931
[11] Paris P, *et al, Fusion Eng. Des.* **98-99** (2015) 1349
[12] Li C, *et al, Spectrochim. Acta B* **160** (2019) 105689
[13] Zhao D, *et al, Nucl. Fusion* **61** (2020) 016025
[14] Gromelski W, *et al, The European Physical Journal Plus*, **136**(5) (2021) 13360-021-01507-8
[15] Dwivedi V, *et al, Nucl. Mater. Energy*, **27** (2021) 100990
[16] Shimada M, *et al, Nucl. Fusion* **47** (2007) S1
[17] Kreter A, *et al, Phys. Scr.* **T159** (2014) 014039
[18] Hakola A, *et al, Phys. Scr.* **T171** (2020) 014038
[19] Suchoňová M, *et al, Nucl. Mater. Energy* **12** (2017) 611-616
[20] Karhunen J, *et al, Phys. Scr.* **159** (2014) 014067
[21] Almaviva S, *et al, Fusion Eng. Des.* **157** (2020) 111685
[22] Paris P *et al, Phys. Scr.* **T170** (2017) 014003
[23] Almaviva S, *et al, Fusion Eng. Des.* **146** (2019) 2087–2091
[24] Malaquies A, *et al, J. Nucl. Mater.* **483** (2013) 208

[25] Russo R E, *et al*, *Anal.Chem.* **85** (2013) 6162−6177
[26] Fishburn J M, *et al Appl. Opt.* **43**(35) (2004) 6473-6476
[27] Veis P, *et al*, *Phys. Scr.* **T171** (2020) 014073
[28] Almaviva S, *et al*, *Spectrochim. Acta B.* **181** (2021) 106230
[29] Dwivedi V, *et al*, *Eur. Phys. J. Plus*, (2021), submitted
[30] Almaviva S, *et al*, *Fusion Eng. Des.* **96**–**97** (2015) 848–851
[31] Karatodorov S, *et al*, EMSLIBS (2019): ISBN 978-80-88195-13-9
[32] Babushok V I, *et al*, *Spectrochim. Acta B* **61** (2006) 999-1014
[33] Gąsior P, *ACTA PHYSICA POLONICA* **138**(4) (2020) https://doi.org/10.12693/APhysPolA.138.601
[34] Colao F, *et al*, *Spectrochim. Acta Part B* **57** (2002) 1167–1179
[35] Pribula M, *et al*, *Phys Scr*. **T167** (2016) 014045
[36] Kreter A, *et al*, *Fusion Sci. Technol.*, **68** (2015) 8–14
[37] Jiang X, *et al*, *Fusion Eng. Des.* **146** (2019) 96–99
[38] Jiang X, *et al*, *Nucl. Fusion* **61** (2021) 096006
[39] Paris P, *et al*, *Fusion Eng. Des.*, **168**, (2021) 112403
[40] Marín Roldán A, *et al*, *Spectrochim. Acta B* **177** (2021) 106055
[41] Kramida A, *et al*, *NIST LIBS Database* https://physics.nist.gov/PhysRefData/ASD/LIBS/libsform.html
[42] Chichkov B N, *et al*, *Appl. Phys. A* **63** (1996) 109-115
[43] Keller W J, *et al*, *J. Appl. Phys.* **125** (2019) 085103
[44] Paris P, *et al*, *Nucl. Mater. and Energy*, **18** (2019) 1-5
[45] Zhao D, *et al*, *Fusion Eng. Des*. **151** (2020) 111379
[46] Maddaluno G, *et al*, *Nucl. Mater. Energy* **18** (2019) 208
[47] Mazzitelli G, *et al*, *Nucl. Fus.* **51** (2011), 073006
[48] Almaviva S, *et al Fusion Eng. Design* **169** (2021) 112638
[49] Veis P, *et al*, *Nucl. Mater Energy* **25** (2020) 100809
[50] Li C, *et al. Front. Phys.* **11**(6) (2016) 114214
[51] Zhao D, *et al. Rev. Sci. Instrum.* **89** (2018) 073501
[52] Huber A, *et al. Fusion Eng. Des.* 86 (2011) 1336–1340
[53] Vukolov K Yu, *et al. Physics of Atomic Nuclei* **81**(7) (2018) 1008-1014
[54] Laan M, *et al*. *Fusion Eng. Design* **121** (2017) 296-300
[55] Jõgi I, *et al. J. Nucl. Mater* **544** (2021) 152660
[56] Zhao D, *et al*, *J. Anal. At. Spectrom.* **35** (2020) 2867-2879
[57] Cheng-Hsiang L, *et al*, *Meas. Sci. Technol.* **21** (2010) 025307